Iran University of Science and Technology

International Journal of Automotive Engineering

Journal Homepage: ijae.iust.ac.ir

ISSN: 2008-9899

Thermal behavior of a commercial prismatic Lithium-ion battery cell applied in electric vehicles

Y. Salami Ranjbaran [1], M.H. Shojaeefard [2], G.R. Molaeimanesh [2*]

[1]Research laboratory of automotive fluids and structures analysis, Automotive engineering school, Iran University of Science and Technology, Tehran, Iran

[2] Automotive engineering school, Iran University of Science and Technology, Tehran, Iran.

ARTICLE INFO

Article history:

Received : 2 Nov 2017

Accepted: 11 Mar 2018

Published:

Keywords:

Electric vehicles (EVs)

Lithium-ion battery

Dual potential MSMD battery model

Thermal behaviour

Battery performance

A B S T R A C T

This paper mainly discusses the thermal behavior and performance of Lithium-ion batteries utilized in hybrid electric vehicles (HEVs), battery electric vehicles (BEVs) and fuel cell electric vehicles (FCEVs) based on numerical simulations. In this work, the battery's thermal behavior is investigated at different C-rates and also contour plots of phase potential for both tabs and volume-monitored plot of maximum temperature inside the computational domain are illustrated. The numerical simulation is done via ANSYS Fluent traditional software package which utilizes the dual potential multi-scale multi-dimensional (MSMD) battery model to analyze the cell discharge behavior and investigate the thermal performance and potential variation(s). The results show that the maximum temperature of battery surface is proportional to the battery discharge rate, i.e., the higher the C-rate, the greater the cell surface temperature. Moreover, an increasing symmetric pattern is noticed for volume monitor of maximum temperature over the simulation period. Finally, it is worth noting that the battery tab potential varies more quickly if the C-rate becomes greater. In fact, the lowest and highest rate of changes are observed for 1C and 4C rate of discharging, respectively.

*Corresponding Author
Email Address:
molaeimanesh@iust.ac.ir

[DOI: 10.22068/ijae.8.2.2700]

1. Introduction

In the recent years, the problem of air pollution and large amount of carbon oxides (mainly CO2) also nitrogen oxides (mainly NO2) coming out of exhaust of internal combustion engines is becoming the most important issue worldwide [1]. On the other hand, the amount of fossil fuel resources is limited and problems mainly caused by greenhouse gasses is clear to everybody. Paying more attention to renewable energy, scientists have developed green cars such as hybrid electric vehicles (HEVs), battery electric vehicles (BEVs) and fuel cell electric vehicles (FCEVs) in order to mitigate the issue and control the amount of toxic gasses emitted [1]. One of the most favorable power sources of aforementioned vehicles are Lithium ion batteries that are famous for long lifecycle, safety and durability [1]. The main drawback of mentioned batteries is that they generate a lot of heat during charge/discharge because of ohmic and entropic heating [2]. This temperature rise during charging/discharging of HEVs, BEVs and FCEVs, may cause thermal runaway in some cases which can be a potential factor for igniting a very dangerous explosion and irreparable human injuries [3]. Therefore, understanding the thermal behavior and discharge performance of Li-ion battery becomes even more necessary.

The high-numbered production of electric devices such as mobile phones and laptops had increased the need for rechargeable batteries [4-5]. Among different kinds of commercial batteries sold globally, the Li-ion batteries have become the most favorable because of better performance, higher efficiency, low rate of self-discharge and production cost [6]. Other features such as higher energy density and low maintenance cost play a great role to make its usage prior to any other kind of electrical power supply. The Lithium-ion battery is a kind of rechargeable battery in which lithium ions depart from the negative electrode to the positive electrode during discharging process and move backward pending charging [7]. These batteries, like other electrochemical cells, consist of two electrodes and an electrolyte material. In addition, usually the positive electrode or cathode is made up of a lithium compound, such as lithium cobalt oxide and the negative electrode, or anode is made up of carbon and there is a separating layer between them. Usually, the electrolyte in lithium-ion batteries is composed of the lithium salt in an organic solvent [7].

In recent years, many researchers have experimentally and numerically investigated the methods of heat generation of Li-ion batteries by considering a hot wall as a battery inside their research (for instance, a wall with constant temperature of 330 K through the entire simulation) but a little was done to study the thermal behavior and discharge performance of the cell itself through ANSYS Fluent. In this paper, one common commercial Lithium ion battery which is widely used in green vehicle car plant’s industry is simulated via ANSYS Fluent and its thermal behavior, discharge performance (cell voltage variation versus time) and phase potential variation of both positive and negative tabs for different C-rates are being investigated in detail. To sum up, one should mention that the innovation aspect of this research is numerically simulating the overall behavior of commercial Lithium-ion battery in which the chemical reactions inside the battery are also considered (not presented here). On the other hand, this model seems to be more appropriate for those kinds of simulations possessing battery inside. As it will be presented in the following, the battery surface temperature varies significantly and the idea of simulating the battery by a wall with constant temperature is no longer logical.

2. Computational domain and governing equations

Fig. 1 presents the dimensions of the simulated battery (typically called computational domain). In this figure, the dimensions of electrodes and also tabs are presented in detail.

[DOI: 10.22068/ijae.8.2.2700]

This battery is a 14.6 Ah Li-ion battery which is assumed to generate constant amount of heat if discharged at constant C-rates [8].

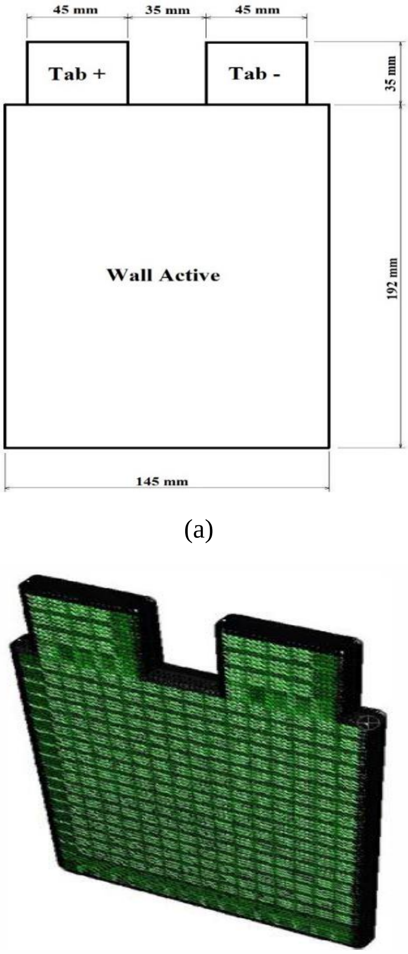

(a)

(b)

Figure 1: (a) Schematic of Lithium-ion battery cell applied in the current simulation (The units are in millimeters) and (b) 3D meshing of 14.6 Ah commercial prismatic Li-ion battery cell.

In this research, the numerical simulation was done via ANSYS Fluent traditional software package. This software utilizes the finite volume technique in order to solve the dominant equations and predict the results. The governing equations are such that consider all mechanisms of heat transfer such as conduction, convection and radiation. In order to accurately investigate the chemical, thermal and electrical behavior of battery, the ANSYS proposes two subsequent models, single potential empirical battery model (SPEBM) or dual potential multi scale multi-dimensional (DPMSMD) battery model. In the current investigation, the latter is being used in order to make results closer to reality and lower the computational costs [9].

The single potential empirical battery model (SPEBM) has a confined capability to investigate the whole variety of electrochemical phenomena in the battery systems, particularly those systems having intricate geometry. The dual potential multi-scale multi-dimensional (MSMD) battery model solves these restrictions by utilizing a homogeneous model appertaining to a multi-scale multi-dimensional approach and deals with various physics in different solution domains. It is important to note that MSMD method includes three electrochemical submodels as follows [9]:

a) The Newman, Tiedemann, Gu and Kim model (known as NTGK).

b) Equivalent circuit model (known as ECM).

c) Newman's Pseudo 2D model (known as Newman's P2D model).

The following mathematical differential equations are solved when applying the NTGK model [8-10]:

$$\frac{\partial \rho\, c_p T}{\partial t} - \nabla.(k\nabla T) = \sigma_+ (\nabla \emptyset)_+{}^2 + \sigma_- (\nabla \emptyset)_-{}^2 + q_{\dot{ECH}} + q_{sh\dot{o}rt} \quad (1)$$

And also:

$$\nabla.(\sigma_- \nabla \varphi_-) = j_{ECH} - j_{short} \quad (2)$$

$$\nabla.(\sigma_+ \nabla \varphi_+) = -j_{ECH} + j_{short} \quad (3)$$

where σ_+ and σ_- represent the effective electrical conductivities for positive and negative electrodes, φ_+ and φ_- show phase

[DOI: 10.22068/ijae.8.2.2700]

potentials for positive and negative tabs, j_{ECH} stands for volumetric current transfer rate, $\dot{q_{ECH}}$ is electrochemical reaction heat due to electrochemical reactions and finally, j_{short} and $\dot{q_{short}}$ show current transfer rate and heat generation rate due to battery internal short circuit.

Through employing the finite element method, the potential and current density distribution on electrodes were investigated and outcomes demonstrated that the aspect ratio of electrodes, the size and location of current collecting tabs have a great effect on the performance of the cell. The NTGK battery model is a simple semi-empirical electrochemical model which is mainly used recently. In the model formulization, the transfer rate of volumetric current is related to the potential field by:

$$j_{ECH} = aY[U - (\varphi_+ - \varphi_-)]$$
(4)

where the parameter *a* is the specific area of electrode sheet also *Y* and *U* are the model parameters. Phase potentials for positive and negative electrodes and also current density are seen in these equations. *U* and *Y* are subordinates of the battery depth of discharge (DOD) defined below:

$$DoD = \frac{Vol}{3600Q_{Ah}} \int_0^t j dt$$
(5)

In the equation above, *Vol* is volume of battery, *Q* is the battery total electric capacity in Ampere hours and *j* is the current density. *Y* is a specific parameter which is specified by experimental data curve fitting. ANSYS Fluent uses the following relationship for *Y* and *U*:

$$U = a_0 + a_1 DoD + a_2(DoD)^2 + a_3(DoD)^3 + a_4(DoD)^4 + a_5(DoD)^5$$
(6)

$$Y = b_0 + b_1 DoD + b_2(DoD)^2 + b_3(DoD)^3 + b_4(DoD)^4 + b_5(DoD)^5$$
(7)

where *DOD* is depth of discharge, a_0-a_5 and b_0-b_5 are fitting coefficients of experimental data at the temperature of 298 K. The electrochemical reaction heat is calculated from the equation below:

$$\dot{q}_{ECH} = j_{ECH}\left[U - (\varphi_+ - \varphi_-) - T\frac{\partial U}{\partial T}\right]$$
(8)

It is worth mentioning that the prime term stands for heat generation due to overpotential phenomenon and the last term lightens up the role of heat generation because of entropic heating.

3. Results and discussion

The following figures will present the phase potential, temperature and voltage variations during battery discharge. Fig. 2 (a) and 2 (b) show the contour plot of phase potential for both negative and positive electrodes for 1C rate of discharging. It can be understood from these two graphs that phase potential in the neighborhood of positive electrode current receiving tab is more than phase potential near the negative current collector of the negative tab. It should be noticed that the reason is mainly because of active material electrical conductivity. The electrical conductivity of active material of the positive electrode is significantly less than that of negative electrode. The phase potential for the positive tab was considered to be 4.3 volts at the beginning and after 3600 seconds, it is predicted to be 3.3384 volts. This illustrate that phase potential of positive tab has been reduced by 0.96 volts, i. e., 22.2 percentage of decrease. The phase potential for the negative tab has been increased for about 0.0032 volts (which was assumed to be near zero at the initiation of the simulation). Finally, one can say that the gradient of maximum phase

[DOI: 10.22068/ijae.8.2.2700]

potential for positive and negative tabs are 3.3416 volts.

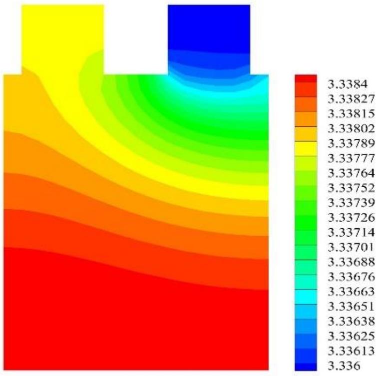

(a)

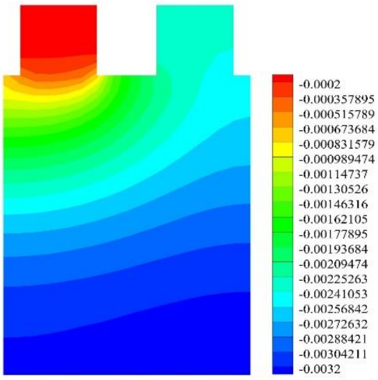

(b)

Figure 2: Contour plot of phase potential for (a) positive electrode and (b) negative electrode for 1C rate of discharge

Fig. 3 presents the contour plot of maximum temperature and also voltage variation of the cell during its affective performance, until it is alive. If the battery is discharged at constant 1C rate, its lifetime would be one hour, 3600 seconds. As it is obvious, the cell voltage decreases from 4.1 volts after simulation initialization to 3.3384 volts at the end of numerical simulation. The software is asked to stop simulation if the cell voltage becomes below 2.7 volts. It is necessary to mention that in practice, if the potential difference becomes below 2.7 volts, the battery experiences heavy damage and even failure. On the other hand, Fig. 3 demonstrates a symmetric pattern in temperature in the whole cell however the discrepancy between temperatures in positive and negative tabs is small and can be neglected. The maximum temperature of the cell's surface after 3600 seconds of battery operation (being discharged at constant rate of 1C) has reached 308.6 K which shows 2.8 percent of increase.

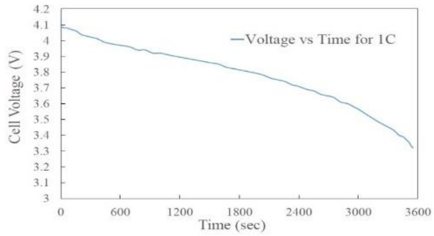

(a)

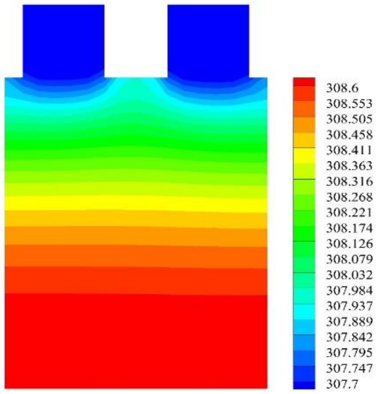

(b)

Figure 2: Contour plot of phase potential for (a) positive electrode and (b) negative electrode for 1C rate of discharge

For the case of 2C rate of discharging, the following figures can be presented. Figs. 4 (a)-(d) represent the contour plot of phase potential for positive and negative tabs, cell voltage variation during 2C rate of discharging and cell surface temperature, respectively. The outcomes reveal that if the battery is being subjected to constant rate of 2C discharging, phase potential for the positive tab decreases from 4.3 volts (at the beginning of the research) to 2.995 volts, which means 32.44 percentage of decrease. On the other hand, phase potential for the negative tab has been increased from almost zero to 0.00661. If this case is being compared with the case of 1C rate of discharging, one may notice that as the C-rate becomes greater, the phase potential of the positive tab experiences more decrease and

[DOI: 10.22068/ijae.8.2.2700]

also phase potential of negative tab grows faster (becomes more negative).

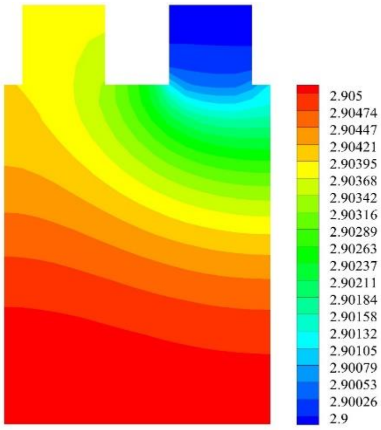

(a)

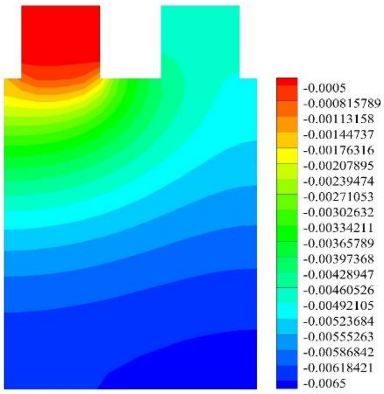

(b)

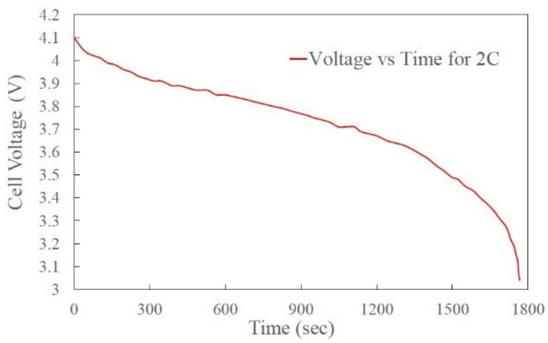

(c)

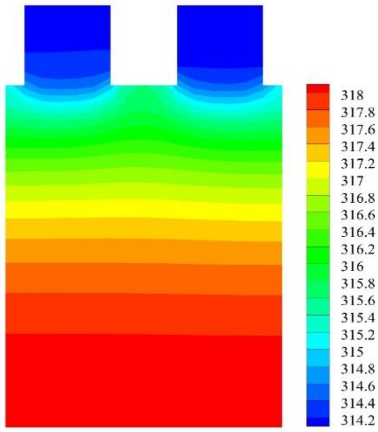

Figure 4: Contour plots of phase potential for (a) positive electrode, (b) negative electrode, (c) cell voltage variation and (d) maximum cell temperature for 2C rate of discharging.

Comparing the contour plots for these two rates of discharging, it can be inferred that if the discharge C-rate becomes greater, the phase potential for positive tab experiences a significant decrease (3.34 is changed to 2.91) and also phase potential for the negative tab becomes larger in magnitude. Another important outcome is about cell voltage variation along simulation period. It can be illustrated from figures that if the C-rate is greater, the voltage variation curve tends to decrease more willingly. It can be derived from the figures that the C-rate plays a great role in the temperature and voltage variation behaviors.

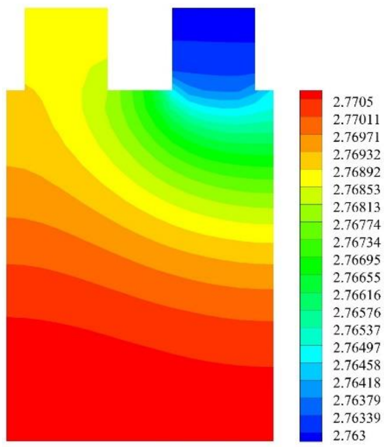

(a)

[DOI: 10.22068/ijae.8.2.2700]

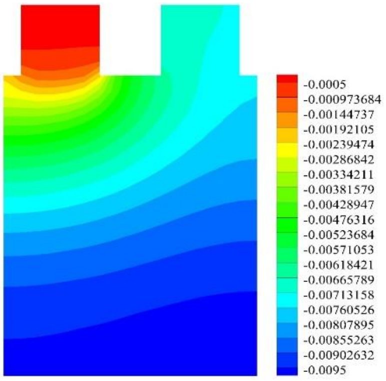

(b)

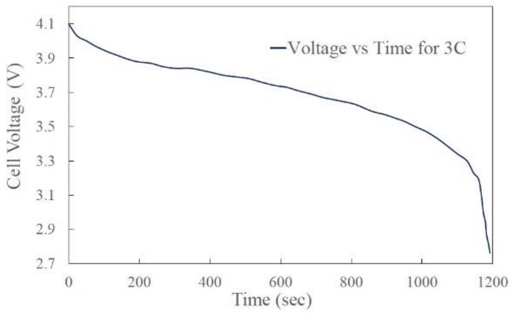

(c)

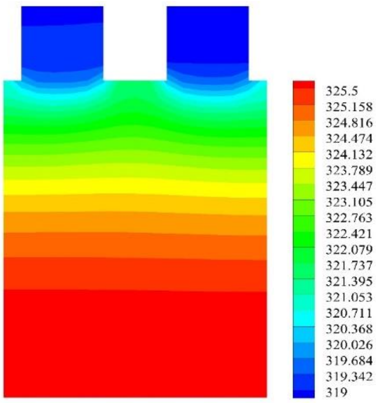

(d)

Figure 5: Contour plot of phase potential for (a) positive electrode, (b) negative electrode, (c) cell voltage variation and (d) maximum cell temperature for 3C rate of discharging.

Moreover, similar figures can be illustrated for 3C and 4C rate of battery discharging. They are presented in Figs. 5 and 6. If these two following plots are compared, one can notice that as stated before, the cell voltage variation happens much more quickly for 4C in comparison with 3C. In other words, the cell voltage varies from 4.1 volts to 2.7705 volts in 1200 seconds after simulation for 3C rate of discharging but its variation is from 4.1 volts to 3.25 volts after 900 seconds. It should be mentioned that if the battery had that much energy to stay alive until 1200 seconds, the phase potential would definitely be below 2.7705 (the case of 3C rate of discharging). If more attention is paid, one can notice that the voltage variation curve has dropped earlier for 4C rate of discharging as stated among comparing the cases of 1C and 2C. Another result is about the maximum temperature occurring inside the computational domain. By looking carefully, one observes that maximum surface temperature of cell has reached 318.8 K for 3C rate of discharging which means that cell’s surface temperature has soared for about 6 percent. For this case, the phase potential of positive tab has been decreased from 4.3 volts to 2.7705 volts which indicates 35.5 percent of decrease. Phase potential of negative tab has been increased from almost zero to 0.0095 volts.

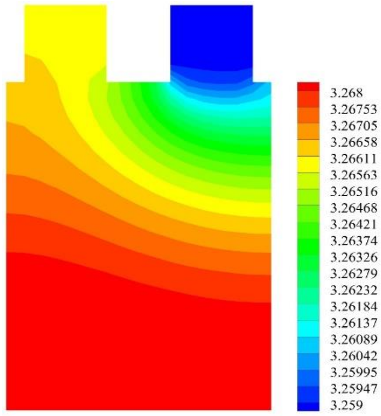

(a)

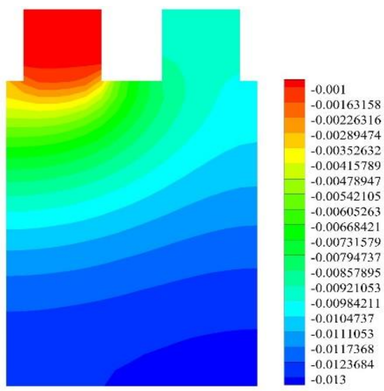

(b)

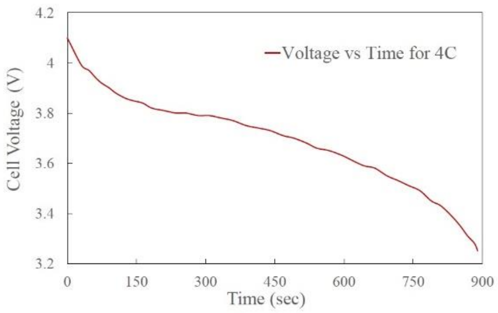

(c)

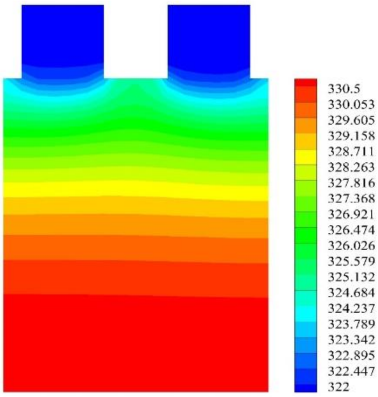

(d)

Figure 6: Contour plot of (a) cell voltage variation and (b) maximum cell temperature for 4C rate of discharging.

As it is obvious, the maximum temperature of cell has increased about 5 degrees for 4C in comparison with 3C. The maximum cell surface temperature has reached 331 K which represents 31 degrees of increase in comparison with the battery temperature at the beginning of the simulation. It becomes clear that the influence of high C-rates on maximum temperature is less than its impact at moderate or low C levels. In other words, changing the C-rate from 1C to 2C increases the maximum temperature 11 degrees Kelvin whereas 3C to 4C discharge rate alteration only increases the maximum temperature for only 5 degrees Kelvin. The final important statement is that by increasing the rate of discharge, more volume of the cell turns in red, which means the tabs are being more and more infected by the hot temperature of the active zone. In other words, the tabs are the regions which are connected to copper wires to transport electrical charges and provide power, but this heat which is coming closer to them may cause wire fire which demands more attention along with designing battery thermal management systems (BTMSs) such as air-cooled, liquid-cooled BTMSs and those benefiting from phase change materials [11-14].

4. Conclusion

In this research, the numerical simulation was accomplished to analyze the discharge behavior of lithium-ion batteries at various C-Rate conditions. The simulation was performed by ANSYS Fluent to specify the discharge behavior of the cell. The CFD simulation model was employed under different discharge rates (1C, 2C, 3C and 4C).

Volume monitor plot of maximum temperature (VMPMT) in the domain on electrode zone shows a different orientation compared to monitor plot of discharge curve (MPDC) and it demonstrates an increasing trend, approximately with constant rate except for the end of the simulation. By comparing the contour plots for various rates of discharge, it can be inferred that if the discharge C-rate becomes greater, the phase potential for positive tab experiences a significant decrease (the positive tab's phase potential has decreased 22.36%, 32.44%, 35.56% and 24% for the cases of 1C, 2C, 3C and 4C, respectively) and also phase potential for the negative tab becomes larger in magnitude as the C-rate increases.. It can be illustrated from figures that if the C-rate is greater, the voltage variation curve tends to decrease more willingly. Finally, it can be derived from the figures that the C-rate plays a great role in the temperature and voltage variation behaviors of Li-ion batteries. As illustrated before, the maximum battery cell surface temperature becomes 308, 318, 325 and 331 K for 1C, 2C, 3C and 4C discharge current which present 2.66%, 6%, 8.3% and 10.3% of temperature rise respectively.

[DOI: 10.22068/ijae.8.2.2700]

References

[1]. Yufei, Chen, and James W. Evans. "Heat Transfer Phenomena in Lithium/Polymer-Electrolyte Batteries for Electric Vehicle Application." *Journal of Electrochemical Society* (1993): 1833-1838.

[2]. Yufei, Chen, and James W. Evans. "Thermal Analysis of Lithium-Ion Batteries." *Journal of Electrochemical Society* (1996): 2708-2712.

[3]. Wang, B. Gu, and Chin. Y. Wang. "Thermal-Electrochemical Modeling of Battery Systems." *Journal of Electrochemical Society*, (2000): 2910-2922.

[4]. Venkat, Srinivasan, and C.Y. Wang. "Analysis of Electrochemical and Thermal Behavior of Li-Ion Cells." *Journal of Electrochemical Society*, (2003): 98-106.

[5]. Ui. Seong. Kim, Chee. Burm. Shin, and Chi-Su. Kim. "Effect of electrode configuration on the thermal behavior of a lithium-polymer battery." *Journal of Power Sources* (2008): 909-916.

[6]. Ui. Seong. Kim, Chee. Burm. Shin, and Chi-Su. Kim. "Modeling for the scale-up of a lithium-ion polymer battery." *Journal of Power Sources* (2009): 841-846.

[7]. Ki. Hyun. Kwon, Chee. Burm. Shin, Tae Hyuk, Kang and Chi-Su, Kim. "A two-dimensional modeling of a lithium-polymer battery." *Journal of Power Sources* (2006): 151-157.

[8]. Ui. Seong. Kim, Jaeshin. Yi, Chee Burm. Shin, Taeyoung. Han, and Seonyoung. Parkc. "Modeling the dependence of the discharge behavior of the Lithium ion battery on the environmental temperature." *Journal of Electrochemical Society*, (2011): 611-618.

[9]. H, Gu. "Mathematical Analysis of a Zn / NiOOH Cell." *Journal of Electrochemical Society*, (1983): 1459-1464.

[10]. S.C. Chen, C.C. Wan, and Y.Y. Wang, "Thermal analysis of lithium-ion batteries." *Journal of Power Sources* (2005): 111-124.

[11]. M.H. Shojaeefard, G.R. Molaeimanesh, S. Jenabi Haghparast, Y. Salami, "Towards an ultimate method for studying the thermal behavior of Li-ion batteries employed in battery electric vehicles (BEVs), hybrid electric vehicles (HEVs) and fuel cell electric vehicles (FCEVs): A Review." 1st Iran congress on industrial applications of advanced materials and manufacturing (IAAMM), Tehran, 2017.

[12]. M.H. Shojaeefard, G.R. Molaeimanesh, S. Jenabi Haghparast, Y. Salami, "Passive thermal management of Li-ion batteries used in green vehicles via phase change materials (PCMs)." 1st Iran congress on industrial applications of advanced materials and manufacturing (IAAMM), Tehran, 2017.

[13]. M.H. Shojaeefard, G.R. Molaeimanesh, S. Jenabi Haghparast, Y. Salami, "Thermal behavior investigation of Li-ion batteries applied in battery electric vehicles (BEVs), hybrid electric vehicles (HEVs) and fuel cell electric vehicles (FCEVs)." 3rd International Conference on Recent Innovation in Industrial Engineering and Mechanical Engineering, Tehran, 2016.

[14]. M.H. Shojaeefard, G.R. Molaeimanesh, S. Jenabi Haghparast, Y. Salami, "Phase change materials (PCMs) and their application in the industry of battery electric vehicles (BEVs) and hybrid electric vehicles (HEVs)." 3rd International Conference on Recent Innovation in Industrial Engineering and Mechanical Engineering, Tehran, 2016.

[DOI: 10.22068/ijae.8.2.2700]